Colloids and Surfaces B: Biointerfaces 165 (2018) 103–110

Contents lists available at ScienceDirect

Colloids and Surfaces B: Biointerfaces

journal homepage: www.elsevier.com/locate/colsurfb

Albumin-covered lipid nanocapsules exhibit enhanced uptake performance by breast-tumor cells

F. Galisteo-González[a,d,*], J.A. Molina-Bolívar[b], S.A. Navarro[c,d,e,f], H. Boulaiz[c,d,e,f], A. Aguilera-Garrido[a,d], A. Ramírez[e,f], J.A. Marchal[c,d,e,f]

[a] Department of Applied Physics, University of Granada, Spain
[b] Department of Applied Physics II, Engineering School, University of Málaga, Spain
[c] Department of Human Anatomy and Embryology, University of Granada, Spain
[d] Excellence Research Unit "Modeling Nature" (MNat), University of Granada, Spain
[e] Biopathology and Medicine Regenerative Institute (IBIMER), University of Granada, Spain
[f] Biosanitary Research Institute of Granada (ibs.GRANADA), University Hospitals of Granada-University of Granada, Spain

ARTICLE INFO

Article history:
Received 24 November 2017
Received in revised form 6 February 2018
Accepted 11 February 2018
Available online 13 February 2018

Keywords:
Olive-oil nanocapsules
Curcumin
Drug-delivery system
Cellular uptake

ABSTRACT

Liquid lipid nanocapsules (LLN) represent a promising new generation of drug-delivery systems. They can carry hydrophobic drugs in their oily core, but the composition and structure of the surrounding protective shell determine their capacity to survive in the circulatory system and to achieve their goal: penetrate tumor cells. Here, we present a study of LLN covered by the protein human serum albumin (HSA) and loaded with curcumin as a hydrophobic model drug. A cross-linking procedure was performed to further strengthen the protective protein layer. Physicochemical properties and release kinetics of the nanocapsules were investigated, and cellular uptake and killing capacity were evaluated on the human breast-cancer line MCF-7. The nanocapsules exhibited a half maximal inhibitory concentration (IC_{50}) capacity similar to that of free curcumin, but avoiding problems associated with excipients, and displayed an outstanding uptake performance, entering cells massively in less than 1 min.

1. Introduction

Controlled drug delivery may be considered a frontier area of pharmaceutical science and technology, involving a multidisciplinary scientific approach and contributing significantly to human health care. New delivery systems, compared to conventional ones, can improve efficacy and patient compliance and convenience. Due to the poor solubility of most anticancer drugs, current therapies must use solubilizer agents for intravenous administration, which provoke unpleasant secondary effects. Nanoparticle-based drug-delivery systems are suitable to overcome this solubility problem while offering other advantages, such as a high degree of biocompatibility and versatility [1], sustained delivery [2], and protection from chemical and physical degradation [3]. An important restriction for the use of nanoparticles (NP) in drug delivery is their potential toxicity [4]. A proposed solution for this limitation is to adopt, as nanocarriers, proteins that exit in the human body, such as albumin. Human serum albumin (HSA), adsorbed onto polystyrene nanoparticles, reportedly inhibits their phagocytosis and promotes prolonged circulation time in blood [5–7]. Therefore, HSA is considered a disopsonin, i.e. a molecule that can avoid clearance by the reticulo-endothelial system. On the other hand, albumin accumulates in malignant and inflamed tissues, and serves as the main nutrient for tumor growth [8]. For these properties, HSA has been proposed as an important tool to develop drug vehicles [9–11].

Lipid-based nanocarriers are being widely used for drug delivery, with some already passed for clinical use [12]. Examples for such lipid nanovehicles are solid lipid nanoparticles, nanostructured lipid carriers, and liquid lipid nanocapsules (LLN). LLN are colloidal systems consisting of an oily core covered by a protective polymeric shell. They can reach high drug-encapsulation efficiency due to their hydrophobic nature [13] and reduce tissue irritation at the deposition site due to their polymeric shell [14]. Surfactants and hydrophilic molecules such as chitosan, polyethylene glycol (PEG), poly(lactide-co-glycolide) (PLGA) or poloxamers, have been used to coat LLN [15].

Features such as the pharmacokinetics, biodistribution, and the colloidal stability of NP in biological media are governed largely by their surface properties. Most NP formulations are rapidly

* Corresponding author at: Departamento de Física Aplicada, Campus de Fuentenueva, Universidad de Granada, Spain.
E-mail address: galisteo@ugr.es (F. Galisteo-González).

https://doi.org/10.1016/j.colsurfb.2018.02.024
0927-7765/

sequestered by cells of the mononuclear phagocyte system after intravenous administration. The choice of an appropriate coating polymer to decrease the interaction of the NP with serum components is important to achieve long blood-circulation time [16,17]. Recent studies have shown that the synthetic identity of NP plays an important role in the phagocytic cell uptake [18,19]. In addition, the physicochemical properties of the NP shell should influence the drug-release pattern. Human-serum albumin is a good candidate to be employed as external polymeric shell as it is a natural material with biocompatibility, biodegradability, and non-toxicity. This protein shell can be further strengthened by covalent cross-linking, and specific targeting molecules -that can recognize markers on the surface of cancer cells- may be attached by reaction with carbodiimide.

In a previous publication, we presented an extensive study concerning the influence of processing parameters on the properties of olive-oil nanocapsules stabilized by HSA [20]. The present study describes the development of nanocapsules with an olive-oil core covered by a cross-linked HSA shell. We have evaluated how the physico-chemical properties of these nanocapsules can influence their colloidal stability, drug release profile, and cellular uptake. For a hydrophobic drug model, we have chosen curcumin, a natural product with low intrinsic toxicity but recognized medicinal properties such as anti-oxidant [21], anti-inflammatory [22], anti-Alzheimer's disease [23], and anti-tumoral [24] activity.

2. Materials and methods

2.1. Reagents

Curcumin, coumarin-6, human serum albumin, olive oil, oleic acid, glutaraldehyde (GAD), poloxamer F-127, MTT assay reactive [3-(4,5-dimethylthiazol-2-yl)-2,5-diphenyltetrazolium bromide], 4′,6-Diamidino-2-phenylindole dihydrochloride (DAPI), dimethyl sulphoxide (DMSO), L-glutamine, sodium bicarbonate, Hepes buffer, Nile Red, and penicillin/streptomycin solution were purchased from Sigma-Aldrich (Madrid, Spain). DMEM (Dulbecco's modified Eagle medium), MEM (minimum essential medium), and FBS (heat-inactivated fetal bovine serum) were purchased from Thermo Fisher Scientific (Gibco, Grand Island, NY, USA). All aqueous solutions were prepared using ultrapure water from a Millipore Milli-Q Academic pure-water system.

2.2. Preparation of LLN

LLN were prepared using a solvent-displacement method as previously described [20]. Briefly, as a general working scheme, a solution containing 300 μl of olive oil, 37.5 ml of ethanol and different amounts of curcumin was poured into 40 ml of an aqueous phase containing HSA to form an emulsion. The dispersion became turbid immediately because of the formation of nanocapsules. After 10 min of stirring, 250 μl of a 0.16% solution of GAD was added to the dispersion to cross-link the HSA coating molecules. The mixture was left under continuous stirring over a time period of 15 min at 25 °C. Subsequently, the ethanol was evaporated under vacuum at a temperature of 34 °C in a rotary evaporator and the dispersion thoroughly dialyzed against and low-ionic-strength phosphate buffer at pH 7. Similar LLN were prepared without curcumin to be used as blanks, as well as without the GAD cross-linking process for comparison purposes.

The amount of encapsulated curcumin in the nanocarriers was determined by UV–vis spectrophotometry after their disaggregation with propanol. Upon centrifugation at 14,000 rpm for 10 min, the supernatant was collected and the amount of curcumin determined by absorption at 430 nm using a UV–vis spectrophotometer (BioSpectronic Kinetic Spectrophotometer, Eppendorf, Germany). The curcumin concentration was calculated by appropriate calibration curve of free curcumin in propanol ($R^2 > 0.999$). Each batch sample was measured in triplicate.

LLN loaded with the fluorophore coumarin 6 were also prepared to compare the uptake efficiency of nanocapsules with different shells (protein, poloxamer, and a mixture of poloxamer and oleic acid). The preparation method in all cases was the same as previously described, changing curcumin to 0.1 mg of coumarin 6 in the three samples. HSA was replaced by 200 mg of Poloxamer F127 in the PL-C sample, and by 100 mg of Poloxamer F127 and 125 mg of oleic acid in the PLOA-C sample.

2.3. Morphology of nanocapsules

The aspect of LLN was assessed by Cryo-Transmission Electron Microscopy (Cryo-TEM) technique. Five microliters of sample were placed on a glow-discharged holey-type carbon-coated grid (Quantifoil R2/2), and vitrified in liquid ethane using a Vitrobot Mark IV (FEI), under controlled conditions. Samples were maintained at a temperature of approximately −170 °C in liquid nitrogen until they were transferred into a cryo-holder (Gatan), using a cryo-transfer stage. Imaging was carried out using FEI Tecnai G2 20 TWIN transmission electron microscope operating at 120 kV and at a nominal magnification of 100,000–150,000× under low-dose conditions. Images were recorded with a 2k × 2k MP side-mounted CCD camera (Olympus Veleta). Measurements were performed in the Andalusian Centre for Nanomedicine and Biotechnology, BIONAND (Málaga, Spain).

2.4. Measurement of size and surface potential of LLN

The particle-size distribution and zeta potential of LLN were determined by dynamic light scattering (DLS) using a Zetasizer Nano-S system (Malvern Instruments, UK). The self-optimization routine in the Zetasizer software was used for all measurements, and the zeta-potential calculated according to the Smoluchowsky theory. After a 100-fold dilution with a low ionic strength (2 mM) phosphate buffer at pH 7, measurements were performed at 25 °C in triplicate.

2.5. Determination of drug-release kinetics

The in vitro release kinetics of the curcumin-loaded LLN was undertaken by a dialysis method. For this, 2 ml of nanocapsule suspension was stuffed into a dialysis sac and placed in a 200-ml flask containing phosphate buffer at pH 7.4 in a water bath at 37 °C under magnetic stirring at 300 rev/min. At predetermined time intervals, 50 μl aliquots were extracted from the LLN suspension. The remaining amount of curcumin loaded in the nanocapsules was determined as previously described.

2.6. Cell line and culture conditions

The human breast-cancer MCF-7 cell line (American Type Culture Collection, ATCC) was grown at 37 °C in an atmosphere containing 5% CO_2 with DMEM supplemented with 10% (v/v) FBS, 2% L-glutamine, 2.7% sodium bicarbonate, 1% Hepes buffer, and 1% penicillin/streptomycin solution.

2.7. Uptake studies

With the aim of comparing the effectiveness entering cells of different nanocapsule shells, an initial study was performed with coumarin 6-labeled nanocapsules. For this, MCF-7 (5×10^3) cells were seeded into 6-well plates under the culture conditions

detailed above. After 24 h, cells were fed with fresh medium and treated with coumarin 6-loaded nanocapsules. Cells were incubated with the particles for 30 min and 3 h and then washed twice with phosphate saline buffer (PBS) to remove free nanocapsules. Fresh PBS was added and living cells were analyzed by fluorescent microscopy (Nikon Eclipse Ti-S). Just before the examination, DAPI was added at room temperature and in the dark to stain nuclei DNA. Cells treated with empty nanoparticles were used as controls.

In a later stage, after the observation of the enhanced uptake performance of protein-covered nanocapsules, the uptake of Curcumin-LLN was analyzed by fluorescence confocal microscopy at 1 min and 3 h after exposure of cells to nanocapsules with and without GAD cross-linking. MCF-7 cells (3×10^3/well) were seeded in a μ-Slide 8 Well chambers (ibiTreat, IBIDI) using DMEM as culture medium. After 24 h, LLN with a 10 μM concentration of curcumin were diluted in 200 μl of DMEM and added to the cells. Imaging experiments were conducted with a Zeiss LSM 710 laser-scanning microscope using the tissue culture chamber (5% CO_2,37 °C) with a Plan-Apochromat 63×/1.40 Oil DIC m27. Images were processed with Zen Lite 2012 software.

To further discriminate the nature of the bright accumulations observed in some images, similar experiments were performed including nile red in the nanocapsules. In this case, both fluorophores, namely curcumin and nile red, were excited and recorded at different light wavelengths, as specified in the Supplementary Material.

2.8. Proliferation assays

The effect of curcumin-loaded LLN on cell viability was assessed using the MTT assay. MCF-7 breast-cancer cells were seeded into culture flasks with 75 ml DMEM and 10% of FBS. When confluence was optimal (80%), cells were detached with trypsin/EDTA and seeded into 96-well plates at a concentration of 3000 cells per well. The cells were then treated with curcumin-loaded LLN with and without GAD cross-linking, and free curcumin for three days. Free curcumin was dissolved in DMSO and curcumin LLN were diluted in PBS. Curcumin concentrations of all samples were 0.2, 0.5, 1, 3, 5 and 10 μM in 200 μl of DMEM. The toxicity evaluation was performed by MTT assay according to the protocol. Briefly, the MTT solution was prepared at 5 mg/ml in 1× PBS and then diluted to 0.5 mg/ml in MEM without phenol red. The sample solution in the wells was removed and 100 μl of MTT dye was added to each well. Plates were shaken and incubated for 3 h at 37 °C. The supernatant was removed and 100 μl of DMSO were added. The plates were gently shaken to solubilize the formed formazan. The absorbance was measured using a plate reader at a wavelength of 570 nm. The inhibitory concentration 50 (IC_{50}) values were calculated from dose-response curves by linear interpolation. All of the experiments, plated in triplicate wells, were carried out twice.

2.9. Cytotoxicity confocal fluorescence microscopy assays

MCF-7 cells were seeded at a concentration of 3000, 2000, and 1000 cells per well in two μ-Slide 8 Well. Then each plate was treated with curcumin LLN with and without GAD, respectively, at a concentration of 10 μM. The samples were analyzed after 24, 48, and 72 h by confocal fluorescence microscopy. The wavelengths of excitation and emission employed were 405 and 555 nm, respectively. Images were taken with a Zeiss LSM 710 laser-scanning microscope and processed with Zen Lite 2012 software.

2.10. Statistical analysis

SPSS 7.5 software (IBM, Chicago, IL, USA) was used for all data analyses. Results were compared with Student's *t*-test. All data were expressed as means ± standard deviation (SD). Differences were considered statistically significant at a P value of <0.05.

3. Results and discussion

3.1. Characterization

The nanocapsule structure of LLN with cross-linked HSA was imaged by cryo-TEM (Fig. 1). As can be seen in Fig. 1A, oil nanocapsules have a spheroidal shape and are not aggregated. The cryo-electron micrograph shows isolated protein shells that were covering the nanocapsules and have been broken (Fig. 1B). Clearly, the addition of GAD leads to a cross-linking of the protein shell that looks like a skin or a membrane. The LLN sizes are in line with DLS measurements (diameter of 169 ± 4 nm, PDI 0.19 ± 0.05).

The effect of the treatment of nanocapsules with GAD on their surface charge was analyzed by measuring the zeta potential under different experimental conditions. As a consequence of the cross-linking between the HSA molecules surrounding the oily core, the nanocapsule surface charge should significantly rise, since this covalent reaction occurs between the aldehyde groups in GAD and the protein amino residues. The number of positive charges should then diminish and, as a result, the contribution of negatively charged carboxylic groups should become stronger and the net charge of the nanocapsules should be more negative. In Fig. S2A we show that effectively the zeta potential of LLN with cross-linked

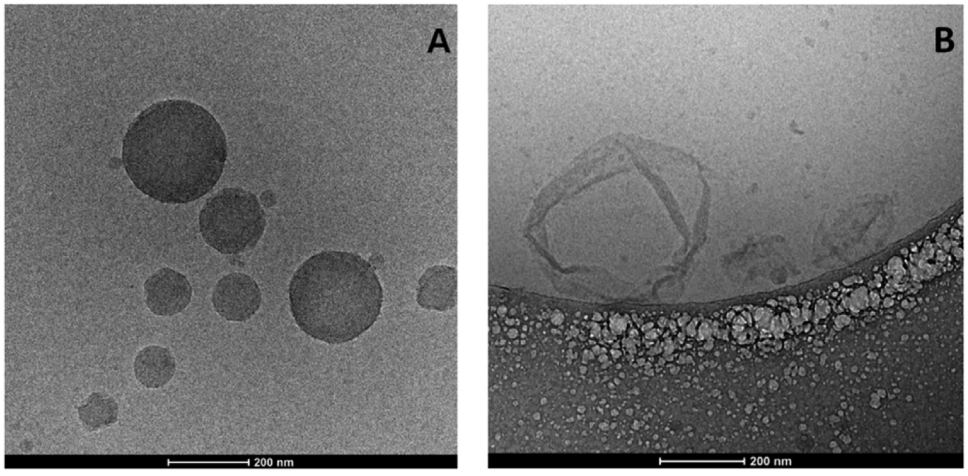

Fig. 1. Cryo-TEM visualization of LLN stabilized by cross-linked HSA.

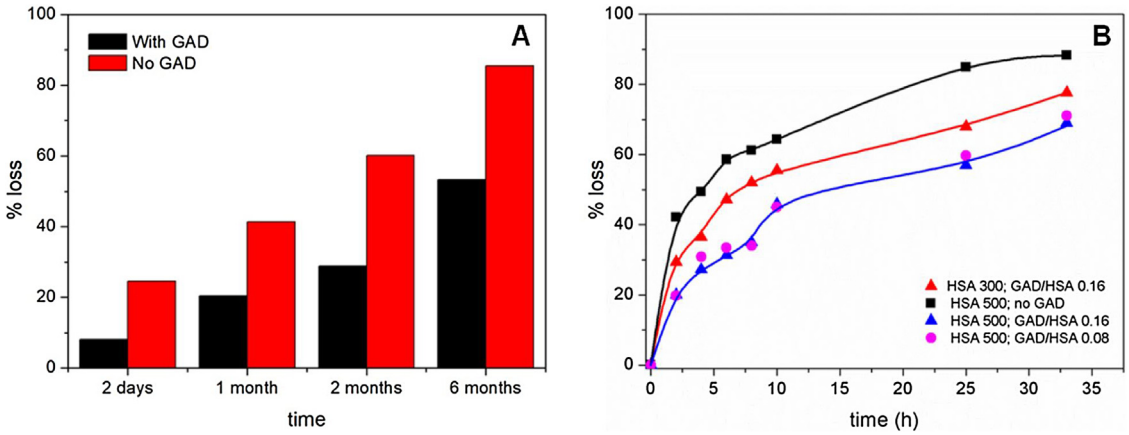

Fig. 2. Percentage loss of curcumin at 4 °C (A) and 37 °C (B) as a function of time.

HSA is more negative at all pH values studied than in the case of LLN not treated with GAD. These results clearly confirm the cross-linking between the HSA molecules. Another approach, leading to the same conclusion, was the evaluation of the effect of different amounts of glutaraldehyde on the zeta potential of LLN (see Fig. S2B).

3.2. Curcumin release properties

In vitro release experiments were performed at two different temperatures, namely 4 °C and 37 °C. The percentage of curcumin lost after storage (4 °C) or conditioning (37 °C) LLN at these two temperatures was evaluated for different time periods. Results for nanocapsules treated and not treated with GAD and kept at 4 °C are presented in Fig. 2A. It is noteworthy that the release of curcumin from LLN with cross-linked HSA is retarded in comparison with non-linked LLN. For these nanocapsules, more than 86% of curcumin was lost after six months, while only 53% of the drug was discharged from LLN covered with a shell of cross-linked HSA. This marked difference suggests that the GAD cross-linked protein behaves as a "protective membrane" to hold the drug molecules inside the nanocapsules.

Another aspect of this study was the investigation of the in vitro curcumin release profile at 37 °C using a dialysis method. Nanocarriers are intended for drug-targeting purposes, and therefore rapid drug release —or an extremely retarded one— may lead to a system failure. Since Cryo-TEM images show that the LLN structure exhibit an oily core surrounded with a protein wall, the curcumin-release profile would be expected to be sensitive to changes in the characteristics of this protein layer. With the aim of analyzing the effect of the GAD content used in the cross-linking reaction on this parameter, the release kinetics for three LLN samples prepared with increasing relation GAD/HSA and with the same amount of HSA were examined. The results in Fig. 2B indicate that nanocapsules with a wall of cross-linked protein molecules retarded the discharge of curcumin at 37 °C, as happened at 4 °C. In other words, the protein cross-linking facilitated the retention of the drug in the nanocapsules.

Nanocapsules not treated with GAD exhibited an initial burst effect more pronounced than LLN with cross-linked HSA. This first stage involved the loss of ca. 42% and 20% of the total entrapped drug amount in the first 2 h for LLN non-treated and treated with GAD, respectively. It is notable that curcumin release profiles for the two GAD/HSA relations studied coincided. These observations suggest that even the smallest amount of GAD used in these experiments is adequate to generate a protective cross-linked protein membrane.

All LLN samples presented a rapid initial release of curcumin. This burst release could be ascribed to an immediate dissolution of curcumin deposited onto the particle surface, or to a drug accumulation near the nanocapsule surface. At a later stage, the curcumin entrapped in the inner nanocapsules core would be discharged more slowly, the rate being determined by the diffusion of the curcumin through the oily phase to the aqueous medium, and probably retarded by the physico-chemical characteristics of the surrounding shell. There was a noteworthy difference in the release kinetics patterns between the protein-covered nanocapsules presented in this study and the surfactant-covered ones described by Abdel-Mottaleb et al. [25]. They reported a linear release of ibuprofen at 37 °C (zero order kinetics), with a total drug discharge after 24 h. By contrast, our system presented a more complex pattern, and drug release did not end even after 33 h. These results suggest that the release mechanism clearly depends upon the nature of the protective nanocapsule shell.

The effect of the HSA content (used in the synthesis of the nanocapsules) on the curcumin release profile at 37 °C is also illustrated in Fig. 2B. As can be seen, the higher the protein concentration, the slower the release kinetics. This result points out to a more compact surface monolayer, or a multilayer (or both), when protein concentration is increased, thereby hampering drug release. At the initial step, the burst release appeared stronger in the LLN prepared with the lower amount of HSA. From these data, we conclude that the initial burst release does not come from curcumin adsorbed at the protein surface, since in that case we would expect a higher burst release with the highest protein concentration. Given these results, it is possible that the first rapid release of the drug is due to the accumulation of curcumin near the LLN surface.

3.3. Cellular uptake of coumarin 6-loaded nanocapsules

As mentioned above in the Material and Methods section, an initial study was performed to compare the effectiveness of different nanocapsule shells entering cells. With that aim, several kinds of LLN were prepared with different surface coverage. For sake of clarity, we present here only two samples: those covered with HSA and with a mixture of Poloxamer F127 and oleic acid.

Fig. 3 shows the fluorescence detected after 30 min of exposure of MCF-7 cells to the samples covered with HSA and poloxamer F127/oleic acid. Green fluorescence corresponds to coumarin 6-loaded nanocapsules, while blue fluorescence highlights cell nuclei. As can be seen, the uptake was significantly faster for the H10-C nanocapsules. After 30 min of incubation, the coumarin 6 was localized in the cytoplasm of cells more abundantly in the case

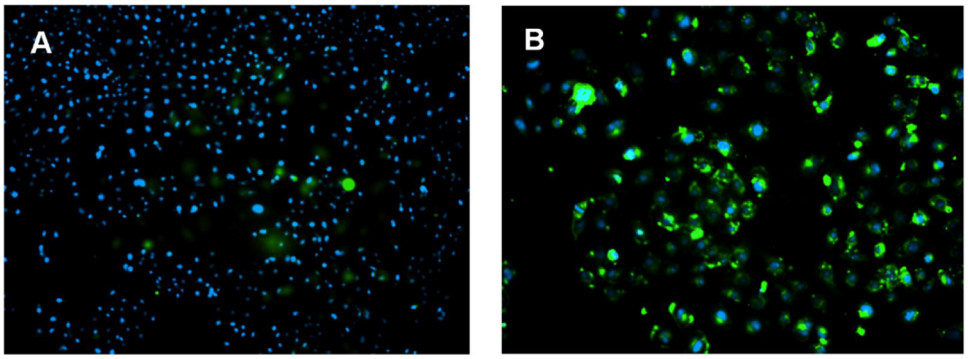

Fig. 3. Uptake assays of MCF-7 cells treated with coumarin 6-LLN during 30 min with two different surface coverages: (A) poloxamer F127/oleic acid; (B) HSA. Cell nuclei are stained with DAPI. Both images ×10 magnification.

of protein-covered nanocapsules (Fig. 3B), indicating that these nanosystems are more effective vehicles to transport molecules within MCF-7 cells. This behaviour may arise from a higher endocytosis rate or a better response to the multi-drug resistance (MDR) efflux mechanism by cell-membrane transport proteins such as p-glycoprotein (P-gp) [26,27].

The difference in internalization among the different nanocapsules may be ascribed to a combination of surface charge and hydrophilicity, which play a major role in the membrane affinity prior to the endocytosis process [28,29]. It has been shown that greater hydrophilicity decreases particle uptake by macrophages as well as nonphagocytic HeLa cells [30]. This is consistent with our results, since the HSA-covered particles presented a more hydrophobic surface than did the sample with Poloxamer F127, and a definitely higher uptake. Moreover, as in the case of *nab*-paclitaxel (an albumin-bound form of paclitaxel), it may be hypothesized that these albumin-covered nanocapsules probably utilizes receptor-mediated albumin endocytosis to internalize cells [31]. Taking into account these different uptake properties attributed to the particle surface, it is noteworthy to mention the possibility of tailoring NP to either prevent or encourage membrane penetration.

In our case, upon observing the enhanced performance of albumin-coated nanocapsules, we continued the study focusing on these systems.

3.4. Cellular uptake of curcumin-LLN

To further elucidate the capabilities of albumin-covered LLN entering MCF-7 cells, and recognize the possible influence of the protein cross-linking procedure, we undertook confocal fluorescence microscopy observations after a very short incubation time (1 min) and a long one (3 h) with HSA-coated LLN with and without GAD treatment. In these experiments coumarin 6 was not included in the LLN formulation, since the model drug used, curcumin, displayed enough fluorescence to be detected in the confocal microscopy. The results are shown in Fig. 4.

As can be seen in this figure, the uptake evaluation reveals an outstanding performance of both types of LLN (with and without GAD cross-linking), entering the cells massively and efficiently in less than 1 min of exposure, and accumulating in the perinuclear zone. Since only a slight difference in fluorescence intensity was detected between the two kinds of nanocapsules within this short time, it suggests that the cross-linking procedure does not influence the (fast) recognition and internalization of the LLN, with cell membranes quickly integrating the nanocapsules into the cytoplasm. As mentioned earlier, this prominent velocity entering cells should be ascribed to the albumin molecules attached to the nanocapsule surface and their natural role as molecular carriers in the mammal bloodstream [31].

Nevertheless, after 3 h of exposure, LLN treated with GAD (Fig. 4D) displayed a clear increase in fluorescence intensity with respect to LLN not treated with GAD (Fig. 4B). To explain this difference at longer exposure times, we invoke the results previously presented for the curcumin-release profiles of both LLN. As stated above (Section 3.2), LLN cross-linked with GAD showed a slower discharge of curcumin at 37 °C (as well as at 4 °C), suggesting that the protein cross-linking facilitates the retention of the drug in the nanocapsules —or, in other words, they display a steadier (and more prolonged) release profile. This slower drug discharge, together with the protection against cytoplasmic digestion afforded by the "hardness" of the cross-linked protein wall, could be responsible for the observed increase in fluorescence intensity with time.

These two characteristics showed by GAD cross-linked LLN, i.e. fast internalization and sustained drug delivery, may represent a great advantage in intracellular uptake and effectiveness compared to other systems that need more time and concentration to be internalized by the cells and offer similar therapeutic response [32].

In order to clarify if the brighter spots shown in Fig. 4D could be ascribed to accumulations of pure curcumin or nanocapsules, an experiment with two fluorophores, namely, curcumin and nile red, was performed. Results are presented in the Supplementary Material, and as it can be observed in Fig. S3A and S3B, both fluorophores present different cytoplasmic distribution patterns, suggesting that nanocapsules have been disrupted and the two compounds have been spread separately. We conclude therefore that the bright accumulations in our experiments are accumulations of pure curcumin inside the cell cytoplasm.

3.5. Proliferation assays

Fig. 5 summarizes the cell-viability data from the MTT assay after treating MCF cells with free curcumin and curcumin-loaded LLN with and without GAD cross-linking. This figure shows that blank (control) LLN, i.e. nanocapsules without curcumin, displayed no toxicity to MCF-7 cells -even in the case of the GAD-treated ones-. Although GAD is strongly toxic to living organisms, the extremely low concentration used (0.004%), the chemical reaction with protein amine groups, and the cleaning process performed thereafter, renders nanocapsules without any appreciable toxicity to cells. In fact, they thrive upon exposure to the LLN, as reflected in the figure (insert). Mahanta et al. have reported that a concentration up to 0.1% GAD (25 times higher than our initial concentration) does not affect viability in normal (HaCaT) and MCF-7 cells [33].

With reference to curcumin-loaded nanocapsules, cell viability declined in all samples tested (Fig. 5). In the case of free curcumin, we found an IC_{50} value of 3.4 ± 0.2 μM, whereas curcumin-LLN with and without GAD cross-linking gave IC_{50} values of 4.3 ± 0.2 and 8.7 ± 0.1 μM, respectively. Although the capacity to kill cells

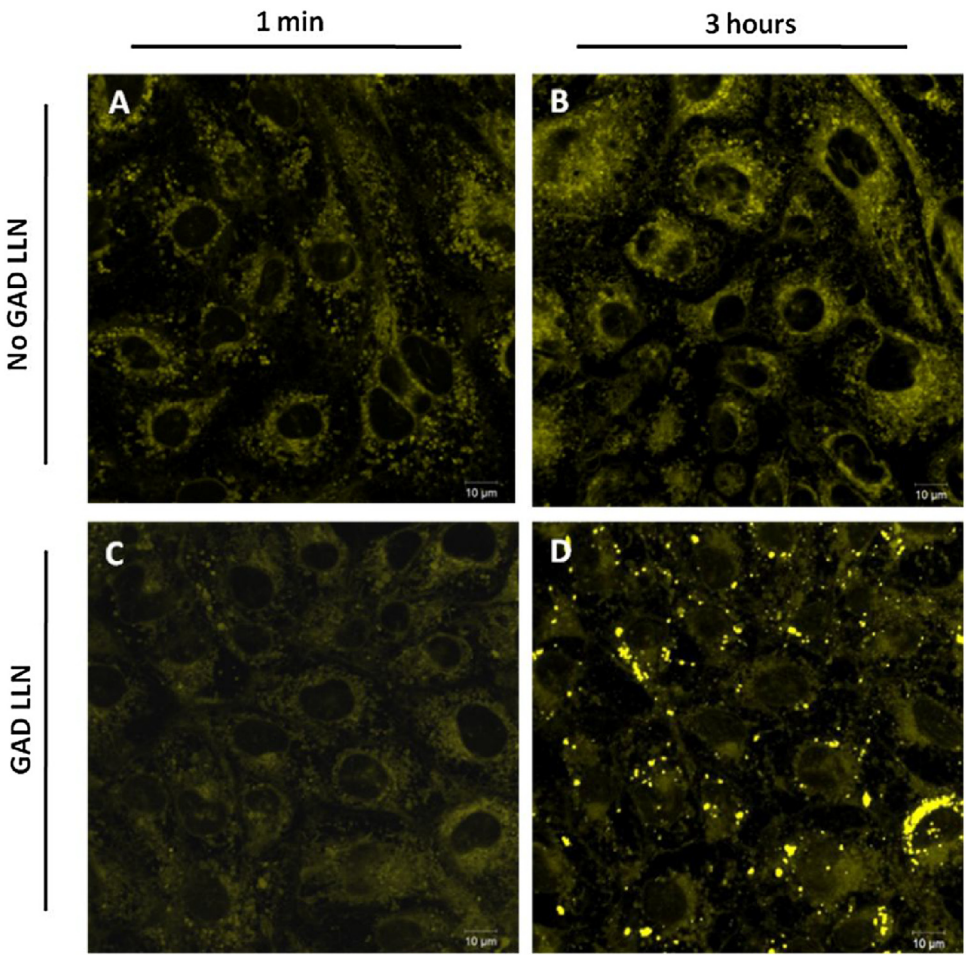

Fig. 4. Confocal fluorescence microscopy after 1 min and 3 h exposure of cells to nanocapsules. LLN without GAD: (A) 1 min, (B) 3 h; LLN cross-linked with GAD: (C) 1 min, (D) 3 h.

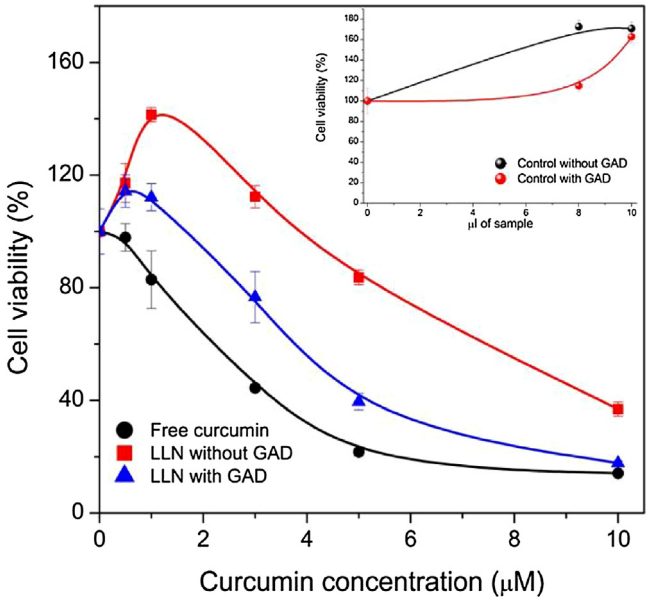

Fig. 5. Cell viability of MCF-7 cells upon treatment with free curcumin and albumin-coated LLN. Insert: Cell viability upon treatment with blank nanocapsules (no curcumin).

decreased slightly in the encapsulated formulation with respect to the (DMSO dissolved) free form, the undoubted advantage of nanocapsules is their ease of dispersion at any concentration in water, and consequently the safety for being administered intravenously, thus avoiding adverse effects of excipients such as Cremophor EL© [34,35]. In this way, the encapsulated formulation would allow the administration of higher amounts of curcumin or other hydrophobic drugs without additional secondary side effects, facilitating a better therapeutic effect and the possibility of greater administration frequency, improving the treatment guidelines. Moreover, as we have previously demonstrated [36], LLN allow high functionalization for vehiculization of targeting molecules like antibodies and other cell-surface active compounds. Other authors have also demonstrated the safety and great utility of these lipid-based nanosystems [37,38].

3.6. Cell-viability assay using confocal fluorescence microscopy

With the aim of gaining insight into the cell-killing process taking place upon exposure to curcumin-loaded nanocapsules, cell viability was analyzed by confocal fluorescence microscopy (Fig. 6). Results show that curcumin-LLN caused cell death after three days of treatment in the MCF-7 human breast-cancer cell line. For LLN not cross-linked with GAD, cells began to die at 24 h after the addition of the nanocapsules (Fig. 6A) and after 72 h (Fig. 6B), cell death increased.

In the case of the GAD cross-linked LLN, cell viability significantly decreased after 24 h of treatment (Fig. 6C). At 72 h (Fig. 6D) the effect persisted and the number of apoptotic cells even rose,

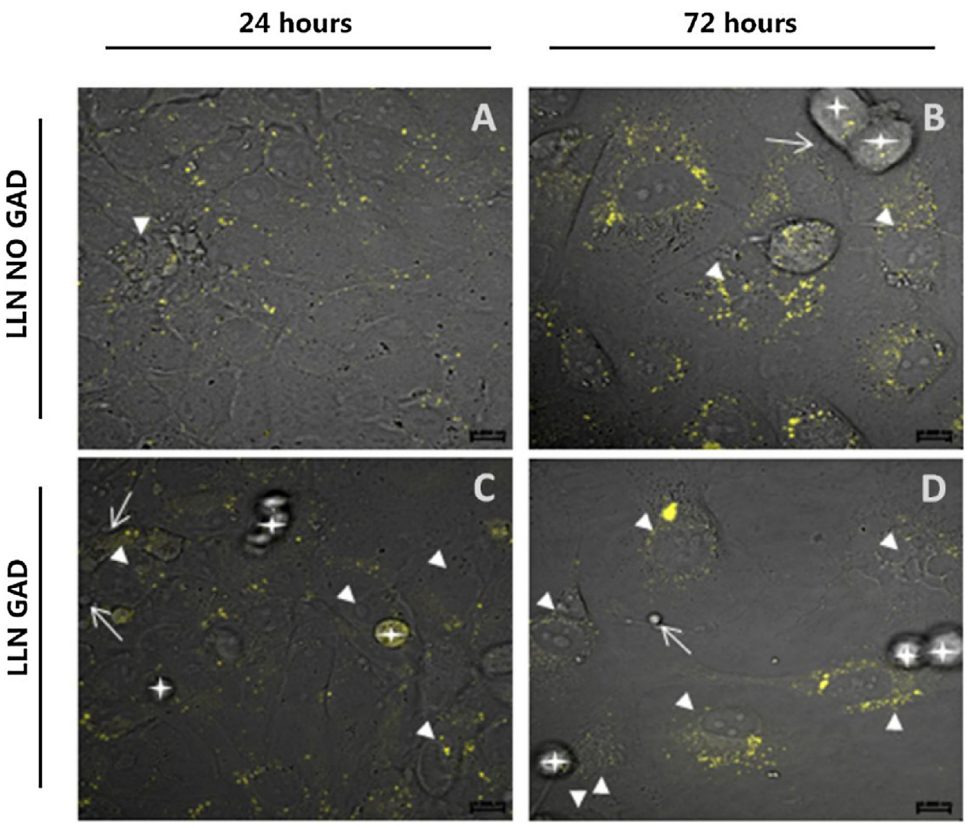

Fig. 6. Confocal fluorescence microscopy of MCF-7 cells in culture: (A-B) non-cross-linked LLN; (C-D) GAD-cross-linked LLN. ▶ Apoptotic cells, → Apoptotic vesicles, ✦ Detached cells.

including the extended formation of large vacuoles, as well as increased cell and nuclear shrinkage, rounding, and detachment.

These apoptotic morphological changes induced by curcumin have been previously described for MCF-7 breast-cancer cells [39], which are deficient in the caspase-activation mechanisms [40,41]. In accordance with the previously described uptake assay, this superior performance of GAD cross-linked LLN may be ascribed to the more continuous and sustained release of curcumin displayed by these kinds of nanocapsules.

4. Conclusions

In the present study, we have developed colloidally stable nanocapsules with an olive-oil core surrounded by a GAD cross-linked HSA shell. The presence of this shell was confirmed by Cryo-TEM and zeta potential studies. In vitro release experiments of encapsulated curcumin showed that the drug:oil relation was key in controlling the drug release from the nanocapsules. A higher ratio resulted in a higher percentage of discharged curcumin with time. The drug released from LLN not treated with GAD was clearly faster than from cross-linked HSA. The increase in the HSA amount used in the preparation of the nanocapsule shell appeared to decrease the rate of curcumin release. A higher protein concentration resulted in a nanocapsule shell with higher density and thickness. Therefore the amount of HSA could be an effective way to control the release of curcumin from LLN.

Albumin-coated nanocapsules displayed better cell-uptake performance than did nanocapsules covered with other surface-active agents (poloxamer and oleic acid), entering MCF-7 cells massively in 1 min. This outstanding performance may be attributed to the more hydrophobic nature of albumin molecules and the specific receptor-mediated endocytosis of this protein.

Curcumin-loaded LLN showed a cytotoxicity capacity slightly lower than free curcumin, but this drawback is clearly overcome by the ease of dispersion of the nanocapsules in aqueous media, allowing administration of hydrophobic drugs at any concentration and rate without the problems associated with emulsifiers like Cremophor EL© and polysorbate 80.

GAD cross-linked albumin-nanocapsules showed better cytotoxicity performance (lower IC_{50} value) than did those covered with non-cross-linked HSA. Confocal fluorescence visualizations supported this enhanced capacity. We hypothesize that this difference in behavior —as a result of the cross-linking procedure— may be due to the slower curcumin release rate displayed by the GAD cross-linked LLN, providing a more sustained drug concentration that cells can cope with less efficiently.

Acknowledgements

This work has been sponsored by the projects MAT2015-62644-C2-1-R and MAT2015-62644-C2-2-R. We thank David Nesbitt for reviewing the English in the manuscript.

Appendix A. Supplementary data

Supplementary data associated with this article can be found, in the online version, at https://doi.org/10.1016/j.colsurfb.2018.02.024.

References

[1] A.R. Madureira, D.A. Campos, P. Fonte, S. Nunes, F. Reis, A.M. Gomes, et al., Characterization of solid lipid nanoparticles produced with carnauba wax for rosmarinic acid oral delivery, RCS Adv. 5 (2015) 22665–22673.

[2] A. Lamprecht, Y. Bouligand, J.-P. Benoit, New lipid nanocapsules exhibit sustained release properties for amiodarone, J. Control. Release 84 (2002) 59–68, http://dx.doi.org/10.1016/S0168-3659(02)00258-4.
[3] A.F. Ourique, A.R. Pohlmann, S.S. Guterres, R.C.R. Beck, Tretionoin-loaded nanocapsules: preparation, physicochemical characterization, and photostability study, Int. J. Pharm. 352 (2008) 1–4.
[4] S. Singh, A. Sharma, G.P. Robertson, Realizing the clinical potential of cancer nanotechnology by minimizing toxicologic and targeret delivery concerns, Cancer Res. 72 (2012) 5663–5668.
[5] L. Thiele, J.E. Diederichs, R. Reszka, H.P. Merkle, E. Walter, Competitive adsorption of serum proteins at microparticles affects phagocytosis by dentritic cells, Biomaterial 24 (2003) 1409–1418.
[6] P. Camner, M. Lundborg, L. Lastbom, P. Gerde, N. Gross, C. Jarstrand, Experimental and calculated parameters on particle phagocytosis by alveolar macrophages, J. Appl. Physiol. 92 (2002) 2608–2616.
[7] K. Ogawara, K. Furumoto, S. Nagayama, K. Minato, K. Higaki, T. Kai, et al., Pre-coating with serum albumin reduces receptor-mediated hepatic disposition of polystyrene nanosphere: implications for rational design of nanoparticles, J. Control. Release 100 (2004) 451–455.
[8] S. Pignatta, I. Orienti, M. Falconi, G. Teti, C. Arienti, L. Medri, M. Zanoni, S. Carloni, W. Zoli, D. Amadori, A. Tesei, Albumin nanocapsules containing fenretinide: pre-clinical evaluation of cytotoxic activity in experimental models of human non-small cell lung cancer, Nanomedicine 11 (2015) 263–273.
[9] C. Bolling, T. Graefe, C. Lübbing, F. Jankevicius, S. Uktveris, A. Cesas, et al., Phase II study of MTX-HSA in combination with cisplatin as first line treatment in patients with advanced or metastatic transitional cell carcinoma, Invest. New Drugs 24 (2006) 521–527.
[10] C. Unger, B. Häring, M. Medinger, J. Drevs, S. Steinbild, F. Kratz, et al., Phase I and pharmacokinetic study of the (6-maleimidocaproyl) hydrazine derivative of doxorubicin, Clin. Cancer Res. 13 (2007) 4858–4866.
[11] N.K. Ibrahim, B. Samuels, R. Page, D. Doval, K.M. Patel, S.C. Rao, et al., Multicenter phase II trial of ABI-007, and albumin-bound paclitaxel, in women with metastatic breast cancer, J. Clin. Oncol. 23 (2005) 6019–6026.
[12] H.I. Chang, M.K. Yeh, Clinical development of liposome-based drugs: formulation, characterization, and therapeutic efficacy, Int. J. Nanomed. 7 (2012) 49–60.
[13] K. Thanki, R.P. Gangwal, A.T. Sangamwar, S. Jain, Oral delivery of anticancer drugs: challenges and opportunities, J. Control. Release 170 (2013) 15–40, http://dx.doi.org/10.1016/j.jconrel.2013.04.020.
[14] C.E. Mora-Huertas, H. Fessi, A. Elaissari, Polymer-based nanocapsules for drug delivery, Int. J. Pharm. 385 (2010) 113–142.
[15] P. Sánchez-Moreno, P. Buzón, H. Boulaiz, J.M. Peula-García, J.L. Ortega-Vinuesa, I. Luque, et al., Balancing the effect of corona on therapeutic efficacy and macrophage uptake of lipid nanocapsules, Biomaterials 61 (2015) 266–278.
[16] C. Fang, N. Bhattarai, C. Sun, M.Q. Zhang, Functionalized nanoparticles with long-term stability in biological media, Small 5 (2009) 1637–1641.
[17] C.D. Walkey, J.B. Olsen, H.B. Guo, A. Emili, W.C.W. Chan, Nanoparticle size and surface chemistry determine serum protein adsorption and macrophage uptake, J. Am. Chem. Soc. 134 (2012) 2139–2147.
[18] S. Zhang, J. Li, G. Lykotrafitis, G. Bao, S. Suresh, Size-dependent endocytosis of nanoparticles, Adv. Mater. 21 (2009) 419–424.
[19] B.D. Chithrani, A.A. Ghazani, W.C.W. Chan, Determining the size and shape dependence of gold nanoparticle uptake into mammalian cells, Nano Lett. 6 (2006) 662–668.
[20] J.A. Molina-Bolívar, F. Galisteo-González, Olive-oil nanocapsules stabilized by HSA: influence of processing variables on particle properties, J. Nanopart. Res. 17 (2015) 391, http://dx.doi.org/10.1007/s11051-015-3192-1.
[21] A. Patel, Y. Hu, J.K. Tiwari, K.P. Velikov, Sysnthesis and characterization of zein-curcumin coloidal particles, Soft Matter 6 (2010) 6192–6199.
[22] R.M. Srivastava, S. Singh, S.K. Dubey, K. Misra, A. Khar, Immunomodulatory and therapeutic activity of curcumin, Int. Immunopharmacol. 11 (2011) 331–341.
[23] T. Hamagushi, K. Ono, M. Yamada, Curcumin and Alzheimer's disease, CNS Neurosci. Ther. 16 (2010) 285–297.
[24] J. Liu, S. Lv, L. Chen, L. Song, S. Guo, S. Huang, Recent progress in studying curcumin and its nano-preparations for cancer therapy, Curr. Pharm. Des. 19 (2013) 1974–1993.
[25] M.A. Abdel-Mottaleb, D. Neumann, A. Lamprecht, In vitro drug release mechanism from lipid nanocapsules (LNC), Int. J. Pharm. 390 (2010) 208–213, http://dx.doi.org/10.1016/j.ijpharm.2010.02.001.
[26] A. Sahu, N. Kasoju, P. Goswami, U. Bora, Encapsulation of curcumin in Pluronic block copolymer micelles for drug delivery applications, J. Biomater. Appl. 25 (2011) 619–639.
[27] V. Anbharasi, N. Cao, S.S. Feng, Doxorubicin conjugated to d-alpha-tocopheryl polyethylene glycol succinate and folic acid as a prodrug for targeted chemotherapy, J. Biomed. Mater. Res. A (2010) 730–743.
[28] A.T. Florence, N. Hussain, Transcytosis of nanoparticle and dendrimer delivery systems: evolving vistas, Adv. Drug Deliv. Rev. 50 (2001) 69–89.
[29] P. Sánchez-Moreno, H. Boulaiz, J.L. Ortega-Vinuesa, J.M. Peula-García, A. Aránega, Novel drug delivery system based on docetaxel-loaded nanocapsules as a therapeutic strategy against breast cancer cells, Int. J. Mol. Sci. 13 (2012) 4906–4919.
[30] K. Kettler, K. Veltman, D. van de Meent, A. van Wezel, A.J. Hendriks, Cellular uptake of nanoparticles as determined by particle properties, experimental conditions, and cell type, Environ. Toxicol. Chem. 33 (2014) 481–492.
[31] H.H. Loong, A. Chan, A.C. Wong, Evolving evidence of the efficacy and safety of nab-paclitaxel in the treatment of cancers with squamous histologies, J. Cancer 7 (2016) 268–275.
[32] J. Wang, R. Zhu, D. Sun, X. Sun, Z. Geng, H. Liu, et al., Intracellular uptake of curcumin-loaded solid lipid nanoparticles exhibit anti-inflammatory activities superior to those of curcumin through the NF-κB signaling pathway, J. Biomed. Nanotechnol. 11 (2015) 403–415.
[33] S. Mahanta, S. Paul, Stable self-assembly of bovine α-lactalbumin exhibits target-specific antiproliferative activity in multiple cancer cells, ACS Appl. Mater. Interfaces 7 (2015) 28177–28187, http://dx.doi.org/10.1021/acsami.5b06076.
[34] H. Gelderblom, J. Verweij, K. Nooter, A. Sparreboom, Cremophor EL: the drawbacks and advantages of vehicle selection for drug formulation, Eur. J. Cancer 37 (2001).
[35] P. Muley, S. Kumar, F. El Kourati, S.S. Kesharwani, H. Tummala, Hydrophobically modified inulin as an amphiphilic carbohydrate polymer for micellar delivery of paclitaxel for intravenous route, Int. J. Pharm. 500 (2016) 32–41, http://dx.doi.org/10.1016/j.ijpharm.2016.01.005.
[36] P. Sánchez-Moreno, J.L. Ortega-Vinuesa, H. Boulaiz, J.A. Marchal, J.M. Peula-García, Synthesis and characterization of lipid immuno-nanocapsules for directed drug delivery: selective antitumor activity against HER2 positive breast-cancer cells, Biomacromolecules 14 (2013) 4248–4259.
[37] Z. He, J. Huang, Y. Xu, X. Zhang, Y. Teng, C. Huang, et al., Co-delivery of cisplatin and paclitaxel by folic acid conjugated amphiphilic PEG-PLGA copolymer nanoparticles for the treatment of non-small lung cancer, Oncotarget 6 (2015) 42150–42168.
[38] X. Wang, X. Chen, X. Yang, W. Gao, B. He, W. Dai, et al., A nanomedicine based combination therapy based on QLPVM peptide functionalized liposomal tamoxifen and doxorubicin against Luminal A breast cancer, Nanomedicine 12 (2016) 387–397, http://dx.doi.org/10.1016/j.nano.2015.12.360.
[39] Y. Akkoc, O. Berrak, E.D. Arisan, P. Obakan, A. Coker-Gurkan, N. Palavan-Unsal, Inhibition of PI3K signaling triggered apoptotic potential of curcumin which is hindered by Bcl-2 through activation of autophagy in MCF-7 cells, Biomed. Pharmacother. 71 (2015) 161–171, http://dx.doi.org/10.1016/j.biopha.2015.02.029.
[40] S. Kagawa, J. Gu, T. Honda, T.J. McDonnell, S.G. Swisher, J.A. Roth, et al., Deficiency of caspase-3 in MCF7 cells blocks Bax-mediated nuclear fragmentation but not cell death, Clin. Cancer Res 7 (2001) 1474–1480.
[41] M.E. García-Rubiño, A. Conejo-García, M.C. Núñez, E. Carrasco, M.A. García, D. Choquesillo-Lazarte, et al., Enantiospecific synthesis of heterocycles linked to purines: different apoptosis modulation of enantiomers in breast cancer cells, Curr. Med. Chem. 20 (2013) 4924–4934, http://dx.doi.org/10.2174/09298673113206660263.